Available online at www.sciencedirect.com
SCIENCE DIRECT®
Vision Research 44 (2004) 2159–2169
Vision Research
www.elsevier.com/locate/visres

Monochromatic ocular wavefront aberrations in the awake-behaving cat

Krystel R. Huxlin [a,b,*,1], Geunyoung Yoon [a,b,1], Lana Nagy [b], Jason Porter [b], David Williams [a,b]

[a] Department of Ophthalmology, University of Rochester Medical Center, Box 314, 601 Elmwood Avenue, Rochester, NY 14642, USA
[b] Center for Visual Science, University of Rochester, Rochester, NY 14627, USA

Received 22 August 2003; received in revised form 28 January 2004

Abstract

Measurement of wavefront aberrations in human eyes has become a reliable, quantitative way of assessing the optical impact of experimental and corrective ocular manipulations. Wavefront measures have also been performed in several other species, but never in cats, an animal model of choice for many ocular studies. Our goal in this study was to measure wavefront aberrations reliably in live, awake-behaving cats in a manner that is directly comparable to that used in human subjects. Six adult cats (*felis cattus*) were trained to fixate small targets on a computer screen. A compact Shack–Hartmann wavefront sensor was aligned with each animal's pupil center and line of sight during fixation. Wavefront images were then collected from which the cats' ocular aberrations were measured up to tenth order Zernike polynomials over a 6 mm pupil. Results show that cat and human ocular wave aberrations were very similar. Second order Zernike modes accounted for more than 90% of the total wave aberration. In agreement with our observation that cat ocular optics were comparable with those of humans, the half height width of both the cat and human higher order point spread function was about 0.95°. These results form a solid basis for future wavefront sensing studies aiming to quantify the effects of ocular manipulations in experimental animals.

Keywords: Wavefront aberrations; Cat; Human; Optical quality

1. Introduction

Monochromatic ocular aberrations can significantly disrupt the quality of vision. Recent theoretical and technological advances have enabled researchers to measure and correct some of these aberrations. Wavefront sensing technology allows quantification of ocular aberrations, which are expressed as deviations from a perfect spherical or plane wave, of the wavefront generated by a single point source of light at the fovea. These deviations can be broken down into many types of aberrations or Zernike modes which are grouped into different orders (Liang, Grimm, Goelz, & Bille, 1994; Liang & Williams, 1997; Thibos, Applegate, Schwiegerling, Webb, & Members, 2001). The biology of lower order wavefront aberrations such as defocus and astigmatism is relatively well understood and the visual impact of these aberrations is generally large. However, higher order aberrations such as coma, trefoil and spherical aberration, can also decrease the quality of vision, particularly at large pupil sizes (Hjortdal, Olsen, & Ehlers, 2002; Liang & Williams, 1997). Ocular surgeries that disrupt corneal or lens structure often change the magnitude and distribution of ocular aberrations among the different orders (Hjortdal et al., 2002). Even procedures such as laser in situ keratomileusis (LASIK) and photorefractive keratectomy (PRK), which can correct defocus and astigmatism (second order aberrations), often increase higher order aberrations such as coma and spherical aberration (Endl et al., 2001; Mierdel, Kaemmerer, Krinke, & Seiler, 1999; Moreno-Barriuso et al., 2001; Oshika, Klyce, Applegate,

* Corresponding author. Address: Department of Ophthalmology, University of Rochester Medical Center, Box 314, 601 Elmwood Avenue, Rochester, NY 14642, USA. Tel.: +1-585-275-5495; fax: +1-585-473-3411.
E-mail address: huxlin@cvs.rochester.edu (K.R. Huxlin).
[1] Authors contributed equally to this work.

0042-6989/$ - see front matter © 2004 Elsevier Ltd. All rights reserved.
doi:10.1016/j.visres.2004.03.017

Howland, & el Danasoury, 1999; Oshika et al., 2002; Seiler, Kaemmerer, Mierdel, & Krinke, 2000).

Animal models have long been used in ocular research, but to date, it has been difficult to quantify their ocular wavefront aberrations (e.g. Coletta, Toilo, Moskowitz, Nickla, & Marcos, 2003; Kisilak, Campbell, Hunter, Irving, & Huang, 2003; Ramamirtham, Norton, Siegwart, & Roorda, 2003; Ramamirtham et al., 2002). Part of the problem is that accurate measurement of wavefront aberrations requires normal corneal physiology. In particular, adequate hydration in the form of a normal, uniform tear film needs to be maintained while the measurements are taken, otherwise significant changes in wavefront aberrations will result (Koh et al., 2002). Anesthesia seriously compromises the quality and quantity of the tear film since animals are no longer able to blink. Artificial tears and other corneal moisturizers do not replicate the chemical or optical qualities of the natural tear film (Huxlin, unpublished observations). Indeed, our early wavefront measures in anesthetized cats treated with a range of such moisturizers exhibited huge inter-image variability in the magnitude of Zernike terms from the 2nd to the 5th order, both within and between imaging sessions. This variability was so severe that we were not able to interpret the results, an outcome that motivated our work to measure such aberrations in awake, fixating animals.

Accurate measurement of wave aberrations also requires subjects to fixate steadily down the optical axis of a wavefront sensor, an alignment that is difficult to achieve in awake animals. Yet, the ability to conduct such measurements reliably over a long period of time would be extremely advantageous for ophthalmological research. In this study, we have succeeded in using a compact Shack–Hartmann wavefront sensor to measure wavefront aberrations in awake, adult cats trained to fixate small visual targets presented on a computer monitor. The cat is an excellent animal model for ocular research. Relative to other mammals (rabbits, rats, mice, monkeys), feline corneal parameters (curvature, size, thickness, histological structure) are similar to those of humans (reviewed in Hughes, 1977). This is important because the cornea contributes to the majority of the optical aberrations in the eye. Furthermore, the biological reaction of the feline cornea to injury or surgical intervention provides a very good approximation of the human cornea's reaction to such manipulations (Bahn et al., 1982; Jester, Petroll, Feng, Essepian, & Cavanaugh, 1992). The cat is thus often used in studies of corneal healing (Petroll, Cavanagh, & Jester, 1998; Telfair et al., 2000a, 2000b). The ability to quantify optical wave aberrations in normal, adult cat eyes has allowed us to better assess the quality of cat optics than was previously possible and has set the stage for future studies on the optical consequences of ophthalmologic interventions.

2. Methods

2.1. Animals

Data were collected from eight eyes in six young, adult cats, purchased from a commercial vendor. All cats were domestic shorthairs (*felis cattus*), were in good health and there was nothing unusual about their upbringing, appearance or visual performance, other than that they were raised and kept in cages most of their lives. The cats were trained to fixate small spots of light on a computer monitor. The animals were motivated for the training by decreasing their body weight to about 75% of normal. They were maintained at this weight for the duration of the study and received the majority of their daily food intake in the form of pureed beef rewards for fixating spots of light during their daily imaging or training sessions. Following each session, the animals were supplemented with dry cat food, leaf lettuce and a vitamin pill to insure that their body weight remained at about 75%, while maintaining good physical health. On week-ends or days when they did not undergo wavefront sensing, cats were given an amount of dry cat food calculated to maintain them at 75% body weight. Water was continuously available in their home cage. All experiments were carried out according to the guidelines of the NIH Guide for the Care and Use of Laboratory Animals (NIH publication no. 86-23, revised 1987) and of the University of Rochester's Committee on Animal Resources.

2.2. Behavioral training protocol

Under deep surgical anesthesia, each cat was fitted with a head-cap consisting of a set of 8 titanium orthopedic screws (Veterinary Orthopedic Implants Inc.) implanted into the skull and joined together by bone cement (Palacos Bone Cement) into which a brass rod was embedded (Pasternak & Horn, 1991). A subconjunctival search coil was implanted around one eye (Judge, Richmond, & Chu, 1980) and connected to a female plug also embedded into the bone cement of the head-cap. The animals were allowed to recover for two weeks before the onset of behavioral training. During behavioral training, each cat was placed inside a magnetic field generated by a set of 50 cm field coils (Remmel, 1984). Their heads were immobilized using the implanted head-cap while their body was loosely confined in a zippered body suit. Signal from their eye coil was detected and calibrated using an eye coil phase detector (Riverbend Electronics). Eye position was calibrated prior to each daily imaging session by requiring the cat to fixate a small (2×2 pixels or 0.03° visual angle) spot of light on a darkened 19″ ViewSonic PF790 computer monitor located 48 cm from its eyes. Animals were rewarded for positioning their gaze within an

electronically defined, square window, 1°–1.5° in length, centered on the fixation spot (Sparks & Sides, 1974). The animals were trained to maintain fixation within this window for 2–3 s. When they did so successfully, they were rewarded with a squirt of pureed beef. The fixation spot was presented randomly at different locations on the computer monitor, within the central 10° of vision. About 20–30 trials were required to calibrate eye position, by making small adjustments to the signal offset and gain on the eye coil phase detector.

2.3. Compact wavefront sensor

In order to measure wave aberrations in awake cats, a Shack–Hartman wavefront sensor was miniaturized so that it could fit into the psychophysical apparatus used for visual testing of cats. The overall dimensions of the modified sensor (Fig. 1A and B) were small and allowed the apparatus to be aligned onto the visual axis and pupil center of one eye in the cat without obstructing vision through the other eye. A schematic diagram of the compact wavefront sensor (CWS) is shown in Fig. 1C.

A laser diode emitting dim, collimated light at a wavelength of 820 nm produced a beacon source of light on the retina. Light reflected out of the eye from this source was then used to measure the wavefront aberration. An infrared pupil illuminator and pupil camera were used to produce a real time (30 Hz) image of the pupil, which was necessary to align the wavefront sensor to the animal's eye during fixation (see below). The pupil illuminator did not affect pupil size. The lenslet array used to image optical aberrations consisted of over 600 lenslets for a 6 mm diameter aperture. The center-to-center spacing of the lenslets was 200 μm and their focal length was 7.9 mm. The magnification of the optical system was 1:1 at the pupil plane. A CCD camera (DALSA CCD Image Capture Technology) was used to capture the resulting spot array patterns with an exposure time of 400 or 500 ms. A "dark image" was collected at the end of each imaging session to document the noise created by the CCD camera itself. This image was collected while the room lights and computer monitor were turned off and the opening of the wavefront sensor was covered with a piece of black construction paper. This dark image was then subtracted from each spot array pattern obtained from that imaging session.

2.4. Measurement of wave aberrations in fixating cats

Wave aberrations were measured in six right eyes and two left eyes. Images were collected in dim surround illumination while the cats fixated a small spot of light (2×2 pixels) displayed on a computer monitor at a distance of 48 cm from the cat's eyes. The cats' pupils were typically about 12–13 mm in diameter during wavefront

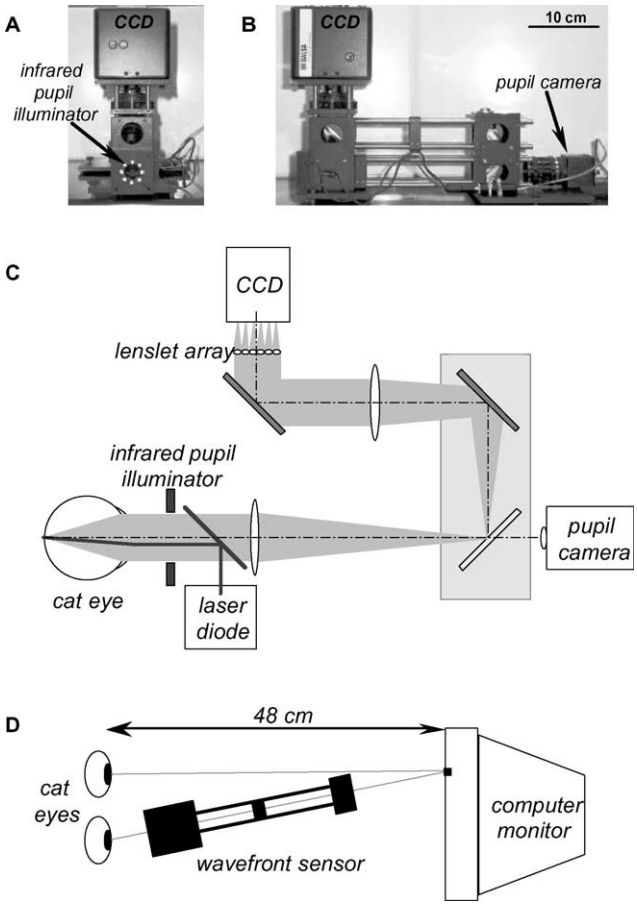

Fig. 1. Miniature Shack–Hartmann wavefront sensor and experimental set-up. (A) Photograph of the wavefront sensor from the front, as seen by the cats during imaging of wavefront aberrations. The infrared pupil illuminator (eight white spots arranged in a circular pattern around the sensor's aperture) and CCD camera are labeled. Under optimal conditions, the cat's line of sight is coaxial with the center of this circle. Note that the wavefront sensor is narrow enough to allow the animal to see to one side of it during imaging of each eye. (B) Side view of the wavefront sensor illustrating the pupil camera which is coaxial with the line of sight. Scale bar of 10 cm applies to both A and B. (C) Optical path inside the wavefront sensor. (D) Schematic diagram illustrating the alignment of the wavefront sensor to the line of sight of one of the cat's eyes during the animal's fixation of a spot of light presented on a computer monitor located 48 cm in front of the cat's eyes.

sensing (Fig. 2). No drugs were used to lubricate the eye, artificially enlarge the pupil or block accommodation. Cats blinked normally during the entire imaging session. Accommodation, though present (see review by Hughes, 1977), was kept relatively constant across cats and imaging sessions by requiring all animals to fixate the same bright spot on the computer screen, which was always placed at the same distance (48 cm) from each animal's eyes and well beyond the near point for the cat (Bloom & Berkley, 1977). The compact wavefront sensor was positioned on a height-adjustable platform between the animal and the computer monitor. For imaging of the left eye, cats repeatedly fixated a spot located at 6° of

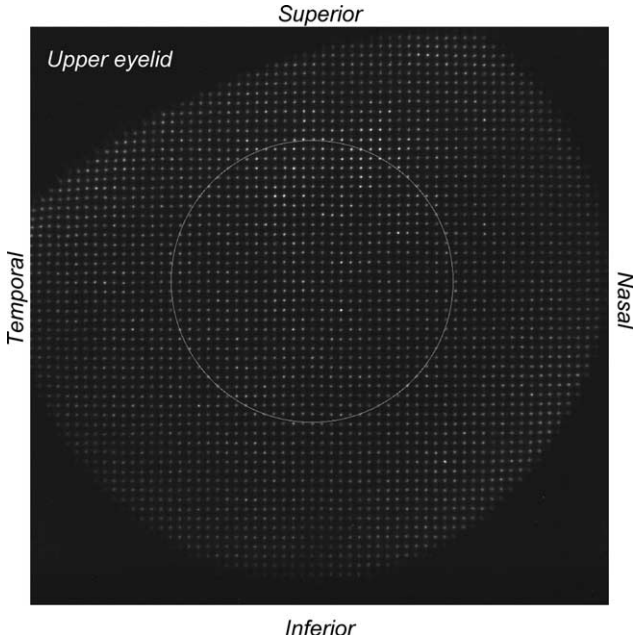

Fig. 2. Typical spot array pattern obtained from an imaging session in a cat. This particular image was taken in the left eye of Cat 2001. Note the oblique shadow in the superior-temporal corner of the image, which prevents light from exiting the eye, and thus, from being detected through the lenslet array. This is part of the cat's upper eyelid, under which no spots of light are found. Throughout the rest of the cat's pupillary aperture, the spots of light recorded by the wavefront sensor's CCD camera are bright and distributed relatively uniformly. A white circle 6 mm in diameter is drawn over the center of the spot array pattern to show the typical aperture over which wave aberrations were analyzed.

visual angle to the right and 6° up from the center of the computer monitor. For imaging of the right eye, cats fixated a spot located 6° to the left and 6° up from the center of the screen. The wavefront sensor was aligned to the visual axis and the center of the pupil in each cat during fixation by centering the live pupil image onto a reference grid displayed on the data acquisition computer's monitor. The distance between the wavefront sensor and the animal's eye was also adjusted slightly until the pupil image was in perfect focus. If debris such as fuzz, dust or excessive ocular secretions, was noticed on the ocular surface, the eye was blinked manually by the experimenter until it disappeared. For each eye, 10–15 spot-array patterns were collected per session. Two to 12 sessions were carried out per eye, each on a different day, to verify repeatability and stability of the measurements.

2.5. Data analysis

Ocular aberrations shift each spot in the spot array pattern from its reference location on the CCD camera, determined by passing a plane wave through the wavefront sensor. The local slope of the wavefront at each lenslet was calculated on the basis of these relative spot displacements. While the cats' pupils were naturally very large under the illumination conditions used in our experiments, the spot array pattern could not be analyzed over a 12–13 mm aperture as the upper eyelid usually occluded part of the pupil (Fig. 2). Because this resulted in a large number of spots missing from the array, wavefront analysis was impossible over the eyelid "shadow". Therefore, while the wavefront sensor has the capacity to measure aberrations over a 12–13 mm pupil, we chose to perform our measurements over a 6 mm aperture, a size that could be attained reliably in all cats, and was consistent with OSA standards for wave aberration measurements in humans (Thibos et al., 2001).

The centration of this 6 mm circular aperture over the spot array patterns was critical to obtaining consistent data. First, a 10 mm circle was drawn and centered on the edges of each spot array pattern. The circle's diameter was then concentrically decreased to 6 mm (see Fig. 2). Within this 6 mm aperture, the center of each spot (centroid) in the spot-array pattern was identified and the two-dimensional displacement of this centroid from the reference spots was measured. Wave aberrations were calculated from these displacements using the Zernike polynomial expansion up to the tenth order. However, only data pertaining to orders two to five are presented here since these orders appear most significant for visual performance. The amplitude of every Zernike term from the second to the fifth order ($j = 3$ through 20—see Table 1 for definition of terms) was expressed in μm. The magnitude of the defocus terms (Z_2^0, $j = 4$) was converted to Diopters using the following formula:

$$\text{Diopter } (D) = \frac{-4\sqrt{3}Z_2^0 \text{ (in } \mu\text{m)}}{(\text{pupil radius in mm})^2}$$

For each eye, the total root mean square (RMS) values for j indices 3–20 were computed and the percentage of the total RMS occupied by lower (2nd) and higher (3rd–5th) order terms were calculated. We also evaluated the weight of each Zernike term (j) in the variance of the ocular wavefront aberration, as follows:

$$\text{Weight } (j) = \frac{j^2}{\sum_{j=3}^{20} j^2} \times 100$$

The two-tailed Student's t-test was used to establish statistical significance.

2.6. Point spread functions (PSFs)

Zernike terms from orders 3–5 were used to calculate the point spread function (PSF) for a 3 mm pupil in each cat eye imaged. The small pupil size was chosen so that the data could be compared with those published previously (reviewed by Hughes, 1977) both for humans (Campbell & Gubisch, 1966; Gubisch, 1967) and anesthetized cats (Bonds, 1974; Enroth-Cugell & Robson,

Table 1
Definition of terms

Zernike term	j index	Classical description
Z_2^{-2}	3	Astigmatism at 45°
Z_2^{0}	4	Defocus
Z_2^{2}	5	Astigmatism at 0° or 90°
Z_3^{-3}	6	y-axis trefoil
Z_3^{-1}	7	y-axis coma
Z_3^{1}	8	x-axis coma
Z_3^{3}	9	x-axis trefoil
Z_4^{-4}	10	Quadrafoil
Z_4^{-2}	11	Secondary astigmatism
Z_4^{0}	12	Spherical aberration
Z_4^{2}	13	Secondary astigmatism
Z_4^{4}	14	Quadrafoil
Z_5^{-5}	15	Pentafoil
Z_5^{-3}	16	Secondary y-axis trefoil
Z_5^{-1}	17	Secondary y-axis coma
Z_5^{1}	18	Secondary x-axis coma
Z_5^{3}	19	Secondary x-axis trefoil
Z_5^{5}	20	Pentafoil

1974; Wassle, 1971). However, because these previously published human PSFs were not calculated from data collected with a wavefront sensor (Campbell & Gubisch, 1966; Gubisch, 1967), wavefront aberrations were measured in eight, randomly selected human eyes using a conventional wavefront sensor (Bausch & Lomb Zywave). Zernike terms were calculated for both 6 and 3 mm pupil sizes. As for the cat eyes, human PSFs were then computed from the 3rd to 5th Zernike orders, over a 3 mm pupil. Experiments were undertaken with the understanding and written consent of each human subject and abided strictly to the Code of Ethics of the World Medical Association (Declaration of Helsinki).

3. Results

3.1. Distribution of optical aberrations in the normal cat eye

As shown in Table 2, the total root mean square (RMS) wavefront error in our sample of eight cat eyes averaged 2.0 ± 1.1 μm (mean ± SD), while higher order RMS (orders 3 through 5) averaged 0.33 ± 0.11 μm, which is in the range of values obtained in humans. Six of the cat eyes were hyperopic (Fig. 3) with defocus ($j = 4$) ranging from −2.1 μm (1.62D) to −1.0 μm (0.77D). Two of the eyes were myopic, with 4.3 μm (−3.31D) and 1.5 μm (−1.15D) of defocus respectively (cats 009 OD and 008 OD—Fig. 3).

Across all cat eyes, the two astigmatism terms were small, averaging 0.007 ± 0.45 μm for $j = 3$ and -0.13 ± 0.50 μm for $j = 5$ (Figs. 3 and 4). Generally, 2nd order terms accounted for about 83% of the eye's total RMS and 95.6% of the total variance of the data (Table 2). Higher order terms (3rd–5th order) accounted for the remaining 17% of the RMS and 4.4% of the variance. Spherical aberration ($j = 12$) was relatively small, averaging 0.018 ± 0.11 μm and accounting for only 0.9% of the total RMS and 5.5% of the higher order RMS. Y-axis coma ($j = 7$) appeared to be one of the more significant higher order aberrations in our sample of cat eyes, averaging -0.11 ± 0.11 μm, which represents 5.6% of the total RMS and 33% of the higher order RMS.

As in humans, the distribution and magnitude of optical aberrations differed between cats (Figs. 3 and 4), and occasionally, between the two eyes of the same cat (compare left and right eyes of Cats 1001 and 2001—Fig. 3). However, all values fell well within the normal range of inter-subject variability seen in humans (Table 2). Furthermore, the small standard deviations obtained for each cat's Zernike term (Fig. 3) demonstrates that there was relatively little variability in a given eye's ocular aberrations, both between the different spot array patterns obtained during a single imaging session, and across many imaging sessions. Within a single imaging session, the mean ± standard deviation of the standard

Table 2
Comparison of cat and human wavefront aberrations

	Cat	Human[a]	Human[b]	Human[c]
Pupil diameter (mm)	6	6	5.7	6
Total RMS (μm)	2.0 ± 1.1	2.2	3.5 ± 3.0	4.5 ± 1.2
3rd–5th order RMS (μm)	0.33 ± 0.11	0.25	0.33 ± 0.11	0.39 ± 0.14
(% total RMS)	16.9 ± 8.8	11.4	9.4	8.8 ± 2.6
2nd order terms (% total variance)	95.6 ± 4.1	∼90	92	99.2 ± 0.5
3rd–5th order terms (% total variance)	4.4 ± 4.1	∼10	8	0.8 ± 0.5

[a] Linear interpolation between 5 and 7 mm pupil data of Castejon-Mochon, Lopez-Gil, Benito, and Artal (2002).
[b] Porter, Guirao, Cox, and Williams (2001).
[c] Human data collected for present study ($N = 8$).

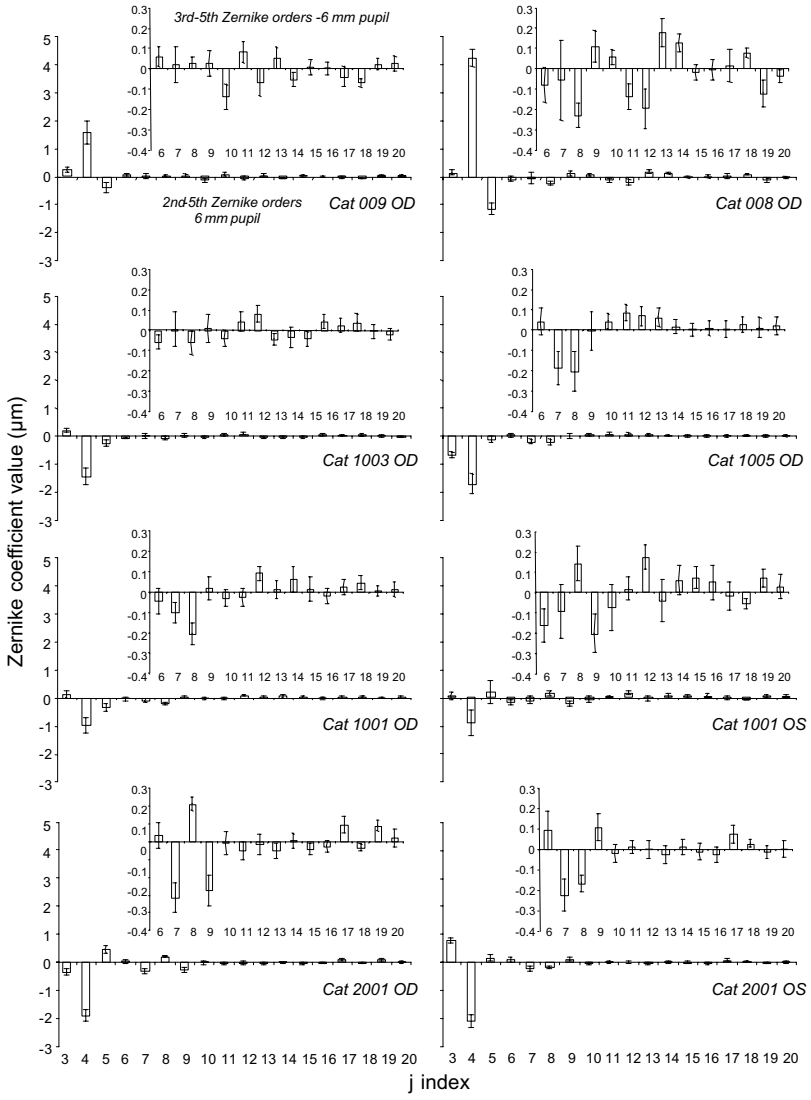

Fig. 3. Plots of mean Zernike coefficient values obtained for each j index from the 2nd to the 5th Zernike orders in each of the eight cat eyes. Data analyzed over a 6 mm pupil were averaged across all images collected for each eye over 2–12 sessions, each on a different day. Cat 009 OD—29 images from three sessions. Cat 008 OD—17 images from two sessions. Cat 1003 OD—26 images from two sessions. Cat 1005 OD—37 images from three sessions. Cat 1001 OD—38 images from three sessions. Cat 1001 OS—24 images from two sessions. Cat 2001 OD—41 images from three sessions. Cat 2001 OS—141 images from 12 sessions. Error bars represent standard deviations of the mean. OD = right eye, OS = left eye. Note the small size of the error bars, demonstrating good repeatability of the measures. Note also the relatively small amounts of higher order aberrations ($j = 6$ through 20), with the exception of y-axis coma ($j = 7$), which is relatively large in five of the eight eyes (1005 OD, 1001 OD and OS and 2001 OD and OS).

deviation of the total RMS calculated for each spot array pattern collected was 0.174 ± 0.099 μm. When data were pooled across different imaging sessions, the standard deviation of the total RMS increased to 0.212 ± 0.169 μm. When data were pooled across all cats, the mean standard deviation of their individual total RMS values increased further to 0.269 ± 0.122 μm. Nevertheless, these standard deviations fall well within the normal range observed in human population studies (see Section 4).

The stability of wave aberrations across time was best demonstrated in cat 2001's left eye (Fig. 3), in which data were collected over twelve different imaging sessions spanning a period of five months. Note that the standard deviations of individual Zernike terms (bottom right graph in Fig. 3) for cat 2001's left eye, though averaged over 141 spot array patterns obtained from twelve days of imaging, were just as small as those in the right eye of this animal (bottom left graph in Fig. 3), for which data were only collected over 41 spot array patterns from three consecutive days of imaging.

Finally, since we were able to image both eyes of cats 1001 and 2001, it was possible to demonstrate the existence of mirror symmetry between the higher order aberrations (3rd through 5th orders) in the two eyes of these animals. Fig. 5 illustrates this phenomenon, which

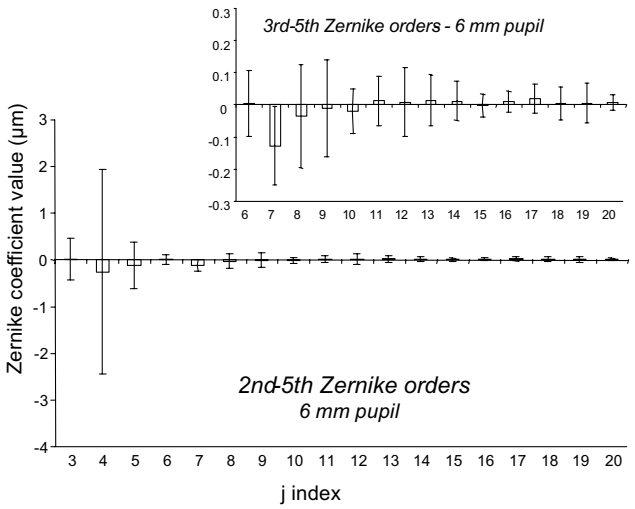

Fig. 4. Mean Zernike coefficient values for individual j indices from the 2nd to the 5th order, averaged over the eight cat eyes and shown for a 6 mm pupil. The inset shows values for higher order terms only (3rd–5th orders), plotted on a different scale. Note that the y-axis coma term ($j = 7$) is the largest of the higher order aberrations.

was seen both in the cats' point-spread functions and wave aberration maps.

3.2. Comparison between cat, human and diffraction-limited PSFs

As shown in Fig. 6, it was possible to calculate PSFs from our wave aberration data over a 3 mm pupil for both humans and cats. When second order terms (defocus and astigmatism) were removed, the PSFs computed from the higher order terms (3rd–5th order) gave cat and human PSFs, RMS and Strehl ratio values that were very similar (Fig. 6A). When the PSFs for the eight cat eyes, the eight human eyes and a diffraction limited system were radially averaged and plotted against minutes of arc (Fig. 6B), the widths at half height of the three curves were identical at 0.95′ arc. While the maximal heights of the human and cat PSFs were lower than the maximal height of the diffraction limited curve, they were not significantly different from each other ($P > 0.05$, Student's t-test).

4. Discussion

4.1. Methodological considerations

Shack–Hartmann wavefront sensors have long been used to measure ocular wave aberrations in the human eye with great precision and reliability (Carkeet, Luo, Tong, Saw, & Tan, 2002; Castejon-Mochon et al., 2002; Liang et al., 1994; Liang & Williams, 1997; Porter et al., 2001). However, performing similar measurements in animals has proven to be difficult (Ramamirtham et al., 2002, 2003; Thibos, Cheng, Phillips, & Collins, 2002). We have successfully developed a paradigm that allows such determinations to be made in awake, fixating cats, a species commonly used for ocular research.

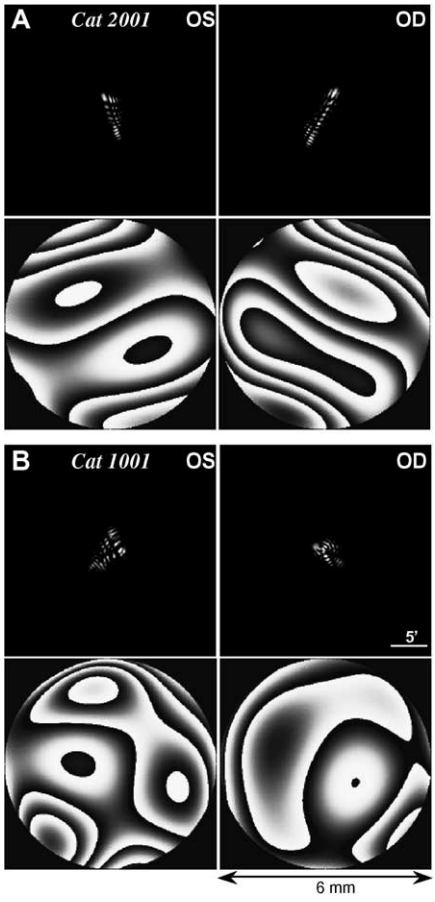

Fig. 5. Mirror symmetry between the higher order aberrations (3rd–5th orders) of the two eyes of individual cats. (A) Mirror symmetry between the two eyes of cat 2001. (B) Mirror symmetry between the two eyes of cat 1001. PSFs (upper rows) and wave aberration maps (bottom rows) were calculated from data measured over a 6 mm pupil diameter. Scale bar = 5′ arc for all PSF images. Scale bar = 6 mm for all wave aberration maps. OD = right eye, OS = left eye.

The issue of maintaining normal corneal physiology and function during wavefront measurements was resolved by using awake animals that blinked and behaved normally. By monitoring eye movements and training cats to fixate, a protocol often used in visual psychophysical experiments (Huxlin & Pasternak, 2004; Pasternak & Horn, 1991; Pasternak & Maunsell, 1992; Pasternak, Thompkins, & Olson, 1995), it was also possible to ensure that animals fixated along the optical axis of the wavefront sensor, as required by the OSA Standardization Committee (Thibos et al., 2001). Not only was our method of alignment consistent with OSA standards for wave aberration measurements (Thibos et al., 2001), but it also resulted in stable data over the many imaging sessions undertaken for this study.

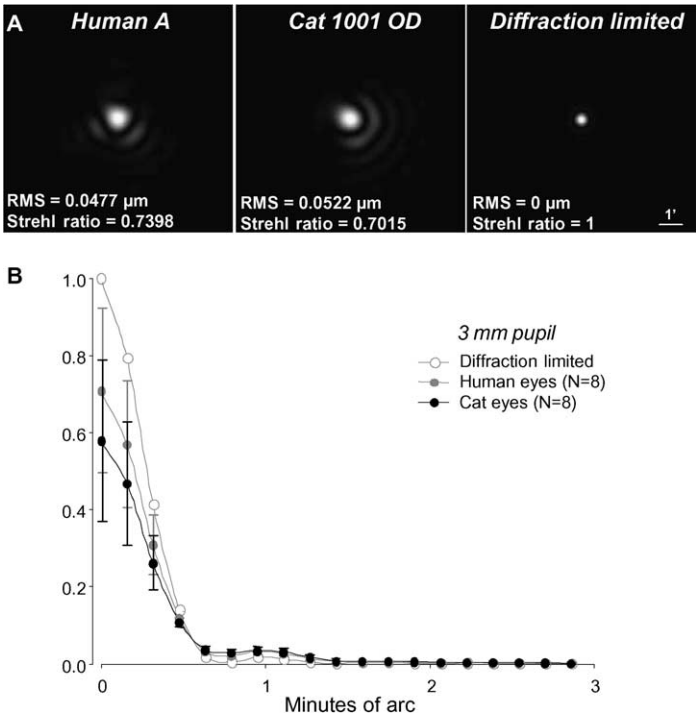

Fig. 6. Comparison of optical quality between the human eye, the cat eye and a diffraction-limited system. (A) PSFs calculated from the higher order wavefront aberrations (3rd–5th orders) over a 3 mm pupil diameter for one of the eight human eyes (Human A), the right eye of cat 1001 and a diffraction limited system where all Zernike terms were set to 0 μm. Scale bar = 1′ arc for all PSF images. The higher order RMS values and Strehl ratios are indicated for each condition. Note the strong similarity in the PSF of the human and cat eye under these conditions. Both are close to being diffraction limited. (B) Plot of the radially averaged PSF, centered on the peak intensity for the diffraction limited condition as well as for the eight human and cat eyes in our sample. Error bars = standard deviations. There is no significant difference between cat and human data in this sample ($P > 0.05$, Student's t-test).

The small variability observed across sessions was most likely due to small differences in the precise alignment of the sensor or to tiny changes in the animals' refractive states. Finally, the mean standard deviation obtained for the RMS wavefront error in our cat population was 0.269 μm, which is comparable to values such as 0.229 and 0.212 μm reported from human population studies (e.g. He et al., 2002).

4.2. Ocular wave aberrations in the normal cat—implications for vision

When measured over a 6 mm aperture and analyzed over the 2nd to the 5th order Zernike polynomials, the ocular wavefront aberrations of cats fell well within the range of values obtained in humans (e.g. Castejon-Mochon et al., 2002; Porter et al., 2001). As in humans, the cat's defocus and the two astigmatism terms, which make up the 2nd order Zernike modes, carry most of the aberration weight, accounting for about 83% of the total RMS value and for over 95% of the total variance. The fact that we found both myopic and hyperopic animals in our small sample suggests that under our testing conditions, there does not seem to be a very a powerful emmetropization mechanism for our population of cats. It is quite possible that wild cats could have a better emmetropization mechanism than our animals, which were specifically bred for research and were raised in cages and artificial lighting all their lives. According to Yinon, the bulk of the evidence suggests that cats, monkeys and chicks raised in small rooms and cages exhibit an increased incidence of myopia relative to normal controls (Yinon, 1984).

Perhaps some of the myopia observed in our cats could result from accommodation during the fixation task. The target that the animals were required to fixate was located 48 cm from their eyes, which would certainly induce an accommodation response. Furthermore, while there is great variability in the reported range of accommodations for the cat eye (from 1*D* to over 10*D*—see Hughes, 1977, for review), there appears to be a suggestions in some of this literature that the physiologic, tonic refractive state of the *awake* cat's eye is slightly myopic (Elul & Marchiafava, 1964). However, it should be noted that we are not making any claims about the absolute refractive power of each cat eye in this study—our main interest is to measure higher order aberrations in the cat eye and to compare them with higher order aberrations in the human eye under similar measurement conditions.

Overall, the cat does not have particularly high levels of higher order aberrations (3rd–5th orders), but as in humans (Howland & Howland, 1977; Porter et al., 2001; Thibos & Cheng, et al., 2002; Walsh, Charman, & Howland, 1984), y-axis coma ($j = 7$, Z_3^{-1}) in the cat accounted for the highest percentage of both the total RMS/variance and of the higher order RMS. In addition, our data showed that cats, just like humans (Liang & Williams, 1997; Porter et al., 2001), can exhibit great similarity in the higher order monochromatic aberrations of their two eyes. This similarity is evidenced by mirror symmetry in their aberration maps, as was shown for cats 1001 and 2001 in Fig. 5.

Contrary to early reports (Bonds, 1974; Bonds, Enroth-Cugell, & Pinto, 1972; Enroth-Cugell & Robson, 1974; Wassle, 1971), the quality of the cat's ocular optics measured with wavefront sensing appears as good as that of the human eye (Campbell & Gubisch, 1966; Gubisch, 1967). Indeed, when using measures of wavefront aberrations over the 3rd to the 5th order Zernike polynomials obtained in this study, it was possible to show that for a 3 mm pupil, the width at half height of the radially averaged PSF did not differ significantly between our sample of eight cat eyes, a sample of eight, randomly chosen human eyes, a diffraction-limited optical system and previously published values for humans (Campbell & Gubisch, 1966; Gubisch, 1967) of about 1′ arc. We attribute the difference in optical quality reported in the present study and those previously reported for the cat (Bonds, 1974; Bonds et al., 1972; Enroth-Cugell & Robson, 1974; Wassle, 1971) to several important factors. First, these previous studies used anesthetized cats. As described earlier, anesthesia compromises the quality and quantity of the tear film, which in itself, induces an increase in higher order optical aberrations (Koh et al., 2002). Secondly, the cats used in these previous studies were fitted with contact lenses, which corrected for defocus but not for astigmatism. Moreover, it has recently been shown that the placement of a corrective contact lens on the cornea can increase higher order optical aberrations (Lu, Mao, Qu, Xu, & He, 2003). Finally, most previous studies of cat optics used a double-pass technique (with the exception of Enroth-Cugell & Robson, 1974) and measured line-spread functions, rather than PSFs. Aside from its precision, one of the many advantages of wavefront sensing is that it allowed us to directly compute the PSF for the measured wave aberrations, something that cannot be done with double-pass techniques (Artal, Marcos, Navarro, & Williams, 1995).

Our findings bring into question the assumption that only visual systems endowed with high resolution need high quality optics. So why does the cat need good optics? Perhaps it needs them for visual detection and discrimination at low light levels. Cats function well in crepuscular and nocturnal environments, and depend highly on vision for hunting and killing prey in these environments (Hughes, 1977). Given that the cat's pupil (Wilcox & Barlow, 1975) can dilate to an area up to three times that achievable in humans (DeGroot & Gebhard, 1952) for the same light levels (Hughes, 1977), cats should experience significantly more optical interference than humans at the same light levels. Perhaps the cat's optics are relatively good because any additional aberrations would significantly degrade this animal's vision to unsustainable levels.

Measures of spatial vision taken at different ambient luminance levels reveal that just as for owls, another nocturnal species, the contrast sensitivity and spatial resolution of cats and humans differ significantly at high, but not low luminance values (Martin, 1982; Pasternak & Merigan, 1981). At a luminance of 16 cd/m^2, the cat's peak sensitivity and acuity were shifted by 2 and 3.5 octaves respectively towards lower frequencies, relative to human values (Pasternak & Merigan, 1981). Over a 6 log unit range of luminance, the cat's sensitivity and acuity decreased by 1 log unit and 1.7 octaves respectively, while human values decreased much more significantly, by 1.7 log units and 5 octaves respectively (Pasternak & Merigan, 1981). The end result is that at low (scotopic) light levels, cat and human contrast sensitivities and acuities are very similar. This is consistent with the findings that brightness increment thresholds in humans and cats are similar at scotopic light levels (Thorn, 1970), but not in high luminance conditions (Berkley, 1976; Mead, 1942). The human/cat comparative study of Pasternak and Merigan (1981) seems to indicate that most of the differences in acuity between humans and cats can be explained by the denser concentration of foveal cones in humans (Osterberg, 1935) and the nearly 1:1 ratio of cones converging to midget ganglion cells (Missotten, 1974). Indeed, cats seem to have about three times larger cone spacing (0.005 mm on the retina or 1.5 min of arc—Steinberg, Reid, & Lacy, 1973) at the retinal area of peak cone density than humans (0.002 mm on the retina or 0.5 min of arc—Polyak, 1957) and a cone-to-beta retinal ganglion cell convergence ratio of about 6–8:1 (Cleland, Harding, & Tulunay-Keesey, 1979; Hughes, 1981; Wassle, Boycott, & Illing, 1981). A more recent psychophysical study comparing the fall off in acuity and contrast sensitivity with retinal eccentricity in the cat (Pasternak & Horn, 1991) revealed a good match with spatial resolution and sensitivity predictions based on the receptive field center sizes and density of beta retinal ganglion cells (Cleland et al., 1979; Hughes, 1981; Wassle et al., 1981).

4.3. Conclusions

In summary, we have combined a psychophysical approach with miniaturization of a Shack–Hartmann

wavefront sensor to quantify wave aberrations in the normal, adult cat eye. By training cats to fixate visual targets, we were able to align the wavefront sensor to their line of sight, while maintaining normal corneal hydration and physiology through natural blinking. This method enabled us to obtain consistent, repeatable measures of Zernike coefficients over a period of time ranging from several days to several months. We found that ocular aberrations in the cat were not significantly different from those in humans, and that feline optics are of relatively high quality. These results are intended to form the basis of future experiments designed to study the effect of ocular manipulations on optical quality in this animal model.

Acknowledgements

The authors wish to thank Drs. Ian Cox and Scott MacRae for stimulating and helpful discussions during the course of this work and for providing the human wavefront measurements. We also thank Emily Brandon for her excellent technical work in behavioral training and testing of the cats. This work was supported in part by a grant from Bausch & Lomb, Inc., the Research to Prevent Blindness Foundation and by CEIS, a NY-STAR-designated Center for Advanced Technology.

References

Artal, P., Marcos, S., Navarro, R., & Williams, D. R. (1995). Odd aberrations and double-pass measurements of retinal image quality. *Journal of the Optical Society of America A, 12*(2), 195–201.

Bahn, C. F., Meyer, R. F., MacCallum, D. K., Lillie, J. H., Lovett, E. J., Sugar, A., & Martonyi, C. L. (1982). Penetrating keratoplasty in the cat. A clinically-applicable model. *Ophthalmology, 89*, 687–699.

Berkley, M. A. (1976). Cat visual psychophysics: Neural correlates and comparisons with man. *Progress in Psychobiology and Physiological Psychology, 6*, 63–119.

Bloom, M., & Berkley, M. A. (1977). Visual acuity and the near point of accommodation in cats. *Vision Research, 17*, 723–730.

Bonds, A. B. (1974). Optical quality of the living cat eye. *Journal of Physiology, 243*, 777–795.

Bonds, A. B., Enroth-Cugell, C., & Pinto, L. H. (1972). Image quality of the cat eye measured during retinal ganglion cell experiments. *Journal of Physiology, 220*, 383–401.

Campbell, F. W., & Gubisch, R. W. (1966). Optical quality of the human eye. *Journal of Physiology, 186*, 558–578.

Carkeet, A., Luo, H. D., Tong, L., Saw, S. M., & Tan, D. T. H. (2002). Refractive error and monochromatic aberrations in Singaporean children. *Vision Research, 42*, 1809–1824.

Castejon-Mochon, J. F., Lopez-Gil, N., Benito, A., & Artal, P. (2002). Ocular wavefront aberration statistics in a normal young population. *Vision Research, 42*, 1611–1617.

Cleland, B. G., Harding, T. H., & Tulunay-Keesey, U. (1979). Visual resolution and receptive field size: Examination of two kinds of cat retinal ganglion cell. *Science, 205*, 1015–1017.

Coletta, N. J., Toilo, D., Moskowitz, A., Nickla, D. L., & Marcos, S. (2003). Wavefront aberrations of the marmoset eye. *Investigative Ophthalmology and Visual Science* (Suppl).

DeGroot, S. G., & Gebhard, J. W. (1952). Pupil size as determined by adapting luminances. *Journal of the Optical Society of America, 42*, 492–495.

Elul, R., & Marchiafava, P. L. (1964). Accommodation of the eye as related to behavior in the cat. *Archives Italiennes de Biologie, 102*, 616–644.

Endl, M. J., Martinez, C. E., Klyce, S. D., McDonald, M. B., Coorpender, S. J., Applegate, R. A., & Howland, H. C. (2001). Effect of larger ablation zone and transition zone on corneal optical aberrations after photorefractive keratectomy. *Archives of Ophthalmology, 119*, 1159–1164.

Enroth-Cugell, C., & Robson, J. G. (1974). Direct measurement of image quality in the cat eye. *Proceedings of the Physiological Society, 239*, 30P–31P.

Gubisch, R. W. (1967). Optical performance of the human eye. *Journal of the Optical Society of America, 57*(3), 407–415.

He, J. C., Sun, P., Held, R., Thorn, F., Sun, X., & Gwiazda, J. E. (2002). Wavefront aberrations in eyes of emmetropic and moderately myopic school children and young adults. *Vision Research, 42*, 1063–1070.

Hjortdal, J. O., Olsen, H., & Ehlers, N. (2002). Prospective randomized study of corneal aberrations 1 year after radial keratotomy or photorefractive keratectomy. *Journal of Refractive Surgery, 18*(1), 23–29.

Howland, H. C., & Howland, B. (1977). A subjective method for the measurement of monochromatic aberrations of the eye. *Journal of the Optical Society of America, 67*(11), 1508–1518.

Hughes, A. (1977). The topography of vision in mammals of contrasting life style: Comparative optics and retinal organization. In *Handbook of Sensory Physiology, V.III/5*. Berlin: Springer Verlag.

Hughes, A. (1981). Cat retina and the sampling theorem; the relation of transient and sustained brisk-unit cut-off frequency to alpha and beta-mode cell density. *Experimental Brain Research, 42*, 196–202.

Huxlin, K. R., & Pasternak, T. (2004). Training-induced recovery of visual motion perception after extrastriate cortical damage in the adult cat. *Cerebral Cortex, 14*, 81–90.

Jester, J. V., Petroll, W. M., Feng, W., Essepian, J., & Cavanaugh, H. D. (1992). Radial keratotomy. 1. The wound healing process and measurement of incisional gape in two animal models using in vivo confocal microscopy. *Investigative Ophthalmology and Visual Science, 33*, 3255–3270.

Judge, S. J., Richmond, B. J., & Chu, F. C. (1980). Implantation of magnetic search coils for measurement of eye position: An improved method. *Vision Research, 20*, 535–538.

Kisilak, M. L., Campbell, M. C. W., Hunter, J. J., Irving, E. L., & Huang, L. (2003). Monochromatic aberrations in the chick eye during emmetropization: Goggled vs control eyes. *Investigative Ophthalmology and Visual Science* (Suppl).

Koh, S., Maeda, N., Kuroda, T., Hori, Y., Watanabe, H., Fujikado, T., Tano, Y., Hirohara, Y., & Mihashi, T. (2002). Effect of tear film break-up on higher-order aberrations measured with wavefront sensor. *American Journal of Ophthalmology, 134*(1), 115–117.

Liang, J., Grimm, B., Goelz, S., & Bille, J. (1994). Objective measurement of the wave aberration of the human eye with the use of a Hartmann–Shack wave-front sensor. *Journal of the Optical Society of America, 11*, 1949–1957.

Liang, J., & Williams, D. R. (1997). Aberrations and retinal image quality of the normal human eye. *Journal of the Optical Society of America, 14*(11), 2873–2883.

Lu, F., Mao, X. J., Qu, J., Xu, D., & He, J. C. (2003). Monochromatic wavefront aberrations in the human eye with contact lenses. *Optometry Vision Science, 80*(2), 135–141.

Martin, G. R. (1982). An owl's eye: Schematic optics and visual performance in *Strix aluco* L. *Journal of Comparative Physiology, 145*, 341–349.

Mead, L. C. (1942). Visual brightness discrimination in the cat as a function of luminance. *Journal of General Psychology, 60*, 223–257.

Mierdel, P., Kaemmerer, M., Krinke, H.-E., & Seiler, T. (1999). Effects of photorefractive keratectomy and cataract surgery on ocular optical errors of high order. *Graefes' Archives of Clinical and Experimental Ophthalmology, 237*, 725–729.

Missotten, L. (1974). Estimation of the ratio of cones to neurons in the fovea of the human retina. *Investigative Ophthalmology and Visual Science, 13*, 1045–1049.

Moreno-Barriuso, E., Lloves, J. M., Marcos, S., Navarro, R., Llorente, L., & Barbero, S. (2001). Ocular aberrations before and after myopic corneal refractive surgery: LASIK-induced changes measured with laser ray tracing. *Investigative Ophthalmology and Visual Science, 42*(6), 1396–1403.

Oshika, T., Klyce, S. D., Applegate, R. A., Howland, H. C., & el Danasoury, M. A. (1999). Comparison of corneal wavefront aberrations after photorefractive keratectomy and laser in situ keratomileusis. *American Journal of Ophthalmology, 127*(1), 1–7.

Oshika, T., Mihyata, K., Tokanuga, T., Samejima, T., Amano, S., Tanaka, S., Hirohara, Y., Mihashi, T., Maeda, N., & Fujikado, T. (2002). Higher order wavefront aberrations of cornea and magnitude of refractive correction in laser in situ keratomileusis. *Ophthalmology, 109*(6), 1154–1158.

Osterberg, G. A. (1935). Topography of the layer of rods and cones in the human retina. *Acta Ophthalmologica, 6*, 11–102.

Pasternak, T., & Horn, K. (1991). Spatial vision of the cat: Variation with eccentricity. *Visual Neuroscience, 6*, 151–158.

Pasternak, T., & Maunsell, J. H. R. (1992). Spatiotemporal sensitivity following lesions of area 18 in the cat. *Journal of Neuroscience, 12*(11), 4521–4529.

Pasternak, T., & Merigan, W. H. (1981). The luminance dependence of spatial vision in the cat. *Vision Research, 21*, 1333–1339.

Pasternak, T., Thompkins, J., & Olson, C. (1995). The role of striate cortex in visual function of the cat. *Journal of Neuroscience, 15*, 1940–1950.

Petroll, W. M., Cavanagh, H. D., & Jester, J. V. (1998). Assessment of stress fiber orientation during healing of radial keratotomy wounds using confocal microscopy. *Scanning, 20*, 74–82.

Polyak, S. (1957). *The vertebrate visual system*. Chicago: University of Chicago Press.

Porter, J., Guirao, A., Cox, I. G., & Williams, D. R. (2001). Monochromatic aberrations of the human eye in a large population. *Journal of the Optical Society of America, 18*(8), 1793–1803.

Ramamirtham, R., Norton, T. T., Siegwart, J. T., & Roorda, A. (2003). Wave aberrations of tree shrew eyes. *Investigative Ophthalmology and Visual Science* (Suppl).

Ramamirtham, R., Roorda, A., Kee, C.-S., Hung, L.-F. F., Qiao, Y., & Smith, E. L. (2002). Wave aberrations in the young monkey eye. *Investigative Ophthalmology and Visual Science* (Suppl).

Remmel, R. S. (1984). An inexpensive eye movement monitor using the scieral search coil technique. *IEEE Transaction on Biomedical Engineering, BME-31*(4), 388–390.

Seiler, T., Kaemmerer, M., Mierdel, P., & Krinke, H.-E. (2000). Ocular optical aberrations after photorefractive keratectomy for myopia and myopic astigmatism. *Archives of Ophthalmology, 118*, 17–21.

Sparks, D. L., & Sides, J. P. (1974). Brain stem unit activity related to horizontal eye movements occurring during visual tracking. *Brain Research, 77*, 320–325.

Steinberg, R. H., Reid, M., & Lacy, P. L. (1973). The distribution of rods and cones in the retina of the cat (*Felisdomesticus*). *Journal of Comparative Neurology, 148*(2), 229–248.

Telfair, W. B., Bekker, C., Hoffman, H. J., Yoder, P. R., Nordquist, R. E., Eiferman, R. A., & Zenzie, H. H. (2000a). Healing after photorefractive keratectomy in cat eyes with a scanning midinfrared Nd:YAG pumped optical parametric oscillator laser. *Journal of Refractive Surgery, 16*, 32–39.

Telfair, W. B., Bekker, C., Hoffman, H. J., Yoder, P. R., Nordquist, R. E., Eiferman, R. A., & Zenzie, H. H. (2000b). Histological comparison of corneal ablation with ER:YAG laser, Nd:YAG optical parametric oscillator, and excimer laser. *Journal of Refractive Surgery, 16*(1), 40–50.

Thibos, L. N., Applegate, R. A., Schwiegerling, J. T., Webb, R. V., & Members, V. S. T. (2001). Standards for reporting the optical aberrations of eyes. In S. M. MacRae, R. R. Kruger, & R. A. Applegate (Eds.), *Customized corneal ablation. The quest for SuperVision* (pp. 348–361). Thorofare: SLACK Incorporated.

Thibos, L. N., Cheng, X., Phillips, J. R., & Collins, A. (2002). Optical aberrations of chick eyes. ARVO.

Thorn, F. (1970). Detection of luminance differences by the cat. *Journal of Comparative Physiological Psychology, 70*, 326–334.

Walsh, G., Charman, W. N., & Howland, H. C. (1984). Objective technique for the determination of monochromatic aberrations of the human eye. *Journal of the Optical Society of America, 1*(9), 987–992.

Wassle, H. (1971). Optical quality of the cat eye. *Vision Research, 11*, 995–1006.

Wassle, H., Boycott, B. B., & Illing, R.-B. (1981). Morphology and mosaic of on- and off-beta cells in the cat retina and some functional considerations. *Proceedings of the Royal Society of London B, 212*, 177–195.

Wilcox, Y. G., & Barlow, H. B. (1975). The size and shape of the pupil in lightly anesthetized cats as a function of luminance. *Vision Research, 15*, 1363–1365.

Yinon, U. (1984). Myopia induction in animals following alteration of the visual input during development: A review. *Current Eye Research, 3*, 677–690.